Cross Talk MAC: a Directional MAC Scheme for Enhancing Frame Aggregation in mm-Wave Wireless Personal Area Networks

Peng Wang and Marina Petrova
RWTH Aachen University, Institute for Networked Systems
Kackertstrasse 9, D-52072 Aachen, Germany
Email: {pwa, mpe}@inets.rwth-aachen.de

***Abstract*—The abundance of unlicensed frequency resources in the mm-Wave frequency range, especially round 60 GHz bands, have a great potential to fulfill the increasing demands of high speed wireless applications. In mm-Wave wireless communication systems, directional transmission technologies become an inherent feature to compensate the high pathloss. The frame aggregation scheme is designed to maximize network throughput and efficiency for packet-based systems by grouping and transmitting multiple packets in a single channel access. In this paper, by jointly considering the benefits of directional transmission and frame aggregation, we propose a paradigm of parallel directional transmission, named cross talk MAC (CTMAC), for enhancing the spatial reuse of mm-Wave directional wireless networks. Enabled by its packet level channel access algorithm, CTMAC allows parallel transmissions even under the strongest interfered topologies to enhance the performance of the mm-Wave wireless personal area network. The numeric results show that the proposed CTMAC dominates the conventional scheme in nearly all scenarios. Especially, CTMAC outperforms the conventional scheme up to 2-fold with good antenna directivity.**

I. Introduction

A large amount of currently unused spectrum exists at mm-Wave frequency band. In particular, at least 6 GHz continuous unlicensed band are available around 60 GHz carrier frequency worldwide, which has a great potential for high speed and short range indoor communications [1], [2]. The IEEE task group has recently finished the IEEE 802.11ad standard to expand wireless local area networks (WLANs) to 60 GHz carrier frequency. The IEEE 802.11ad standard supports up to 7 Gbits/s datarates. The propagation properties of mm-Wave bands are challenging and require us to revisit many medium access concepts [3], [4], [5], [6], [7]. In order to support applicable communications range with high data rates, the directional transmission technologies become an inherent feature of the mm-Wave communication systems. A lot of work has been carried out to study directional transmission technologies in the context of mmW-communication systems, see for example [8], [9], [10]. One approach is to use directional antennas to enhance the spatial reuse, i.e., allowing multiple users to transmit and receive at the same time in their common vicinities. In general, these MAC schemes have a high tolerance of co-channel interference (CCI) outside the mainlobe. However, the interference inside mainlobe is strictly forbidden.

Frame aggregation was first introduced in IEEE 802.11n, and is inherited by the later standards and amendments. It allows the transmitter to send multiple independent frames back-to-back in one channel access. By grouping frames together and using a single PHY header, frame aggregation can greatly reduce the overhead. In this work, we jointly consider the directivity of mmW-communication technologies and the frame aggregation scheme. We propose cross talk MAC (CTMAC) that enables the parallel transmissions even when the stations (STA) are inside the mainlobes of each other. By using the localization and beamforming information, CTMAC utilizes the receiving time of the receiver of an ongoing communicating pair which is significantly prolonged by the frame aggregation, to let another pair of STAs also transmit even in the main beam of the former transmitting STA. In this study, the CTMAC principle is applied and evaluated on top of the IEEE 802.11ad standard. However, it can be widely used by any mm-Wave communication systems, including uncoordinated random access protocols and 5G radio access networks. To the best of our knowledge, this is the first work that explicitly allows parallel transmissions within the mainlobes of the communicating STAs. The rest of this paper is organized as follows: in Section II we describe the IEEE 802.11ad standard with its frame aggregation scheme, and review directional spatial reuse schemes. We propose our MAC protocol in Section III. Finally, in section IV we compare the performance of our protocol with IEEE 802.11ad standard through simulation studies. The paper is finally concluded in Section V.

II. Preliminary Work

In this section, we review the IEEE 802.11ad standard and its frame aggregation scheme and then briefly analyze some of the recent directional MAC studies.

A. IEEE 802.11ad standard and frame aggregation

Unlike the traditional distributed coordination function (D-CF) in legacy IEEE 802.11 standards, the IEEE 802.11ad standard uses a new time domain structure, the beacon interval

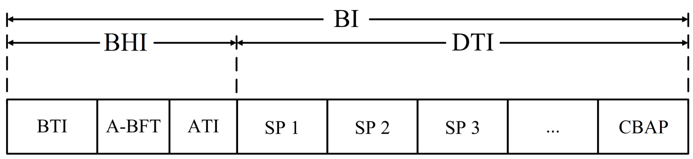

Fig. 1. A general PBSS of IEEE 802.11ad standard and the Beacon Interval.

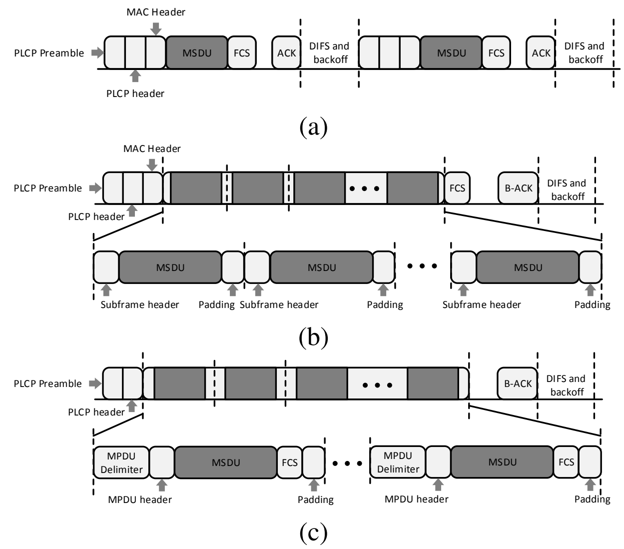

Fig. 2. Frame format of IEEE 802.11ad standard. (a) frame format of normal MPDU; (b) frame format of AMSDU; (c) frame format of AMPDU.

(BI) (Figure 1) as the basic time unit of its Directional Multi-Gigabits (DMG) channel access. A typical BI consists of two major periods, namely the beacon header interval (BHI) and the data transfer interval (DTI). BHI is the first part of a BI and ends before the DTI. BHI can be further subdivided into beacon transmission interval (BTI), association beamforming training (A-BFT) period, and announcement transmission interval (ATI). The group of DMG STAs which are communicating together is defined as a Personal Basic Service Set (PBSS). In a PBSS, A DMG STA is nominated as the PBSS Control Point/Access Point (PCP/AP) which sends the beacon frames in the beginning and organizes the communications in the following BI. In order to synchronize directional STAs, PCP/AP transmits beacon frames for scheduling transmission in BTI, and applies beamforming training during A-BFT. If the antenna training is performed appropriately, all STAs know the directions of their neighboring STAs during the DTI. Finally, data transmissions are carried out during DTI.

The structure of an IEEE 802.11ad frame which is named as PHY layer Protocol Data Unit (PPDU) in the standard is shown in Figure 2(a). It consists of a PHY Layer Convergence Procedure (PLCP) preamble, a PLCP header, a MAC header, a MAC Service Data Unit (MSDU) which is the MAC layer payload, and a checksum sequence. In order to show the transmission efficiency, we use the darker shaded blocks to represent the useful payload, and lighter blocks to mark the control overhead. As shown in Figure 2(a), the overhead of transmitting one MSDU without aggregation is high. Frame aggregation is proposed to reduce the average overhead for each MSDU by grouping them together and then transmitting in one channel access. There are two types of frame aggregation in IEEE 802.11 standards, namely aggregated MAC Protocol Data Unit (AMPDU) and aggregated MSDU (AMSDU). AMPDU is done by first adding a MAC header and generating the checksum sequence to each MSDU to create an MPDU which is the payload of PHY layer, and then transmits multiple MPDUs in a single PPDU. Unlike the AMPDU, AMSDU allows the transmitter to send multiple MSDUs to the same receiver in a single MPDU, i.e., the aggregated MSDUs are transmitted by using only one PHY layer header, one MAC layer header and being proved by one MAC layer checksum sequence.

The most significant difference between AMSDU and AMPDU is the time of performing the MAC layer encapsulation [11]. For AMSDU, the MAC layer encapsulation is done after the aggregation, therefore all encapsulated MSDUs has the same destination address and one checksum sequence. On one hand, its compact structure has a high channel utilization ratio. On the other hand, it has low resistance to the bit error rate because the packet error results in retransmit all MSDUs in the failed AMSDU. In contrast, due to the separately encapsulated MPDU, AMPDU only need to retransmit the collapse MPDU after checking the MPDU individually. Therefore, it is proved in a number of papers that AMPDU performs better than AMSDU in error-prone wireless channels. [12], [13]. The comparison of AMSDU and AMPDU is out of the scope of this study, so we only analyze the frame aggregation scheme by using AMPDU.

B. Directional MACs

The directional wireless transmission is an essential part of the mmW-communication systems. However, a number of new challenges exist when directional technologies and links [14] are employed. A number of mm-Wave directional MAC studies aim at improving the MAC layer of the IEEE 802.11ad standard by exploiting the potential of spatial reuse, which is brought by the directional technologies, i.e., allowing concurrent transmissions according to the interference level. Directional Cooperative MAC (D-CoopMAC) [8] is a relay based mechanism which is designed for for IEEE 802.11ad contention based access period (CBAP) enhancement. D-CoopMAC uses relay STAs to help the STAs which have only pool conductivities. However, it does not consider the sidelobe effects of the directional antenna, which leads to a optimistic estimation of the overall interference level. Due to the imperfect antenna patterns, the sidelobes of the directional antenna and caused CCI may degrade the performance of each communication link when they are carried out concurrently. An interference tolerant link scheduling strategy that enables parallel transmissions in the mm-Wave band is proposed in [9]. It considers the impacts of sidelobes, and uses different modulation and coding schemes (MCS) to optimize the

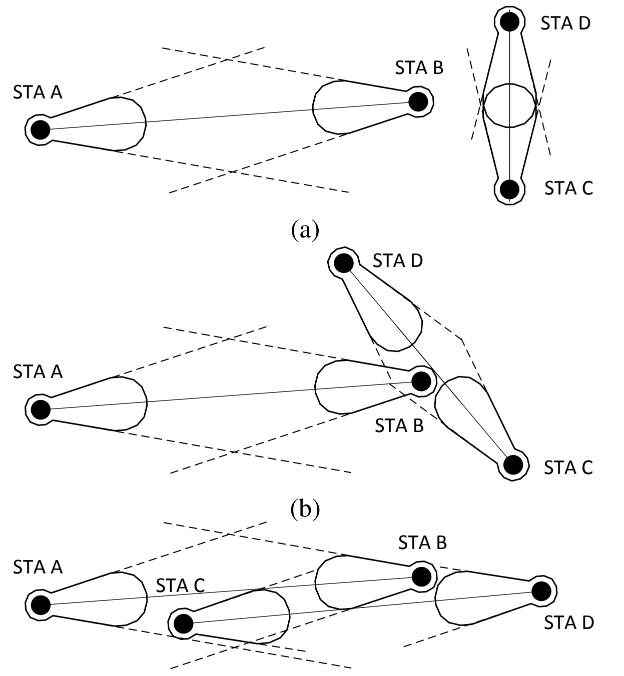

Fig. 3. Three types of interference which are generated by parallel transmissions. (a) sidelobe-sidelobe interference; (b) sidelobe-mainlobe interference; (c) mainlobe-mainlobe interference.

spectrum usage. However, it does not go details of a packet-level medium access algorithm, and also not consider the relations between the performance of parallel transmissions and the topology. Peng et al. proposed CoopDMAC [10], which provides a theoretical analysis between the network topology and performance, while also providing a detailed packet-level protocol design. However, CoopDMAC is a general directional MAC protocol which is not designed for any specific standard, and particularly did not consider mmW-systems.

III. CTMAC Design

In this section, we first analyze the interference level with directional antenna patterns. Based on the interference level analysis, we introduce the principle of CTMAC, and provide a scheduling method can be used for IEEE 802.11ad SP enhancement.

A. Interference analysis

We use a widely used flat-top antenna model [15], [16] which has a mainlobe and sidelobes with unique gain to as the antenna model in this study. As shown in Figure 3, the flat-top antenna has a mainlobe with beamwidth θ and gain $G_{\mathrm{M}} = \eta\frac{2\pi}{\theta}$. The gain out of the main lobe is $G_{\mathrm{S}} = (1-\eta)\frac{2\pi}{2\pi-\theta}$. In this antenna model, the radiation efficiency η [1] is defined in [15], [16] to describe the difference between the gain in the mainlobe and the gain in the sidelobes. According to the antenna model, we can divide the interference scenarios into three types, namely sidelobe-sidelobe (SS) interference, sidelobe-mainlobe (SM) interference, and mainlobe-mainlobe (MM) interference (cf. Figure 3). Most of the existing directional MAC studies allow STAs which are located with SS and SM topologies to carry out concurrent transmissions [9], [10] because the received signal power of MM connections are much higher than the interference power from SS connection or SM connections. For example, consider STA A is transmitting to STA B while STA C is also transmitting to STA D in all three cases in Figure 3. If the antenna training is performed appropriately, the antenna gains of the useful signal transmissions are always the gain of the mainlobe. In this case, the received signal power P_{s} at STA B is

$$P_{\mathrm{s}} = G_{\mathrm{AB}}G_{\mathrm{BA}}PL_{\mathrm{AB}} = 4\pi^2\frac{\eta^2}{\theta^2}\mathrm{PL}_{\mathrm{AB}}, \tag{1}$$

where $\mathrm{PL}_{\mathrm{AB}}$ denotes the pathloss between STA A and STA B. The received interference power P_{i} depends on the directions of the interfering STAs. According to the three topologies shown in Figure 3, the interference power at STA B which is generated from STA C is,

$$P_{\mathrm{i}} = \begin{cases} 4\pi^2\dfrac{(1-\eta)^2}{(2\pi-\theta)^2}\mathrm{PL}_{\mathrm{CB}}, & \text{Fig. 3(a)} \quad (2)\\ 4\pi^2\dfrac{\eta(1-\eta)}{\theta(2\pi-\theta)}\mathrm{PL}_{\mathrm{CB}}, & \text{Fig. 3(b)} \quad (3)\\ 4\pi^2\dfrac{\eta^2}{\theta^2}\mathrm{PL}_{\mathrm{CB}}, & \text{Fig. 3(c)} \quad (4)\end{cases}$$

Thus, the corresponding signal to interference ratio (SIR)[2] is

$$\mathrm{SIR} = \begin{cases} \dfrac{\eta^2(2\pi-\theta)^2}{(1-\eta)^2\theta^2}\dfrac{\mathrm{PL}_{\mathrm{AB}}}{\mathrm{PL}_{\mathrm{CD}}}, & \text{Fig. 3(a)} \quad (5)\\ \dfrac{\eta(2\pi-\theta)}{(1-\eta)\theta}\dfrac{\mathrm{PL}_{\mathrm{AB}}}{\mathrm{PL}_{\mathrm{CD}}}, & \text{Fig. 3(b)} \quad (6)\\ \dfrac{\mathrm{PL}_{\mathrm{AB}}}{\mathrm{PL}_{\mathrm{CD}}}, & \text{Fig. 3(c)} \quad (7)\end{cases}$$

In principle, the directional antennas with high directivity, e.g., the standard gain horn antenna with 25 dBi [18], can provide sufficient SIR to support parallel transmission for SS and SM interference topologies.

A number of studies show that IEEE 802.11 devices are able to find the MCS which can maximize the usage of the SIR and control the packet error rate. For example, Halperin et al. in [19] proposed a packet delivery prediction method. It shows that the transmission parameters, including the MCS, can be accurately predicted based on the channel measurements. Their algorithm is verified on commodity 802.11 NICs based on only the channel information which is read from the device. At least, the rate adaptation algorithm can also be performed

[1] Even through the term radiation efficiency is defined in IEEE Standard for Definitions of Terms for Antennas [17] as the ratio of the total power radiated by an antenna to the net power accepted by the antenna from the connected transmitter, we stick to the definition of radiation efficiency in [15], [16] to improve the readability.

[2] Due to the relatively high interference level [7], noise is ignored in this study

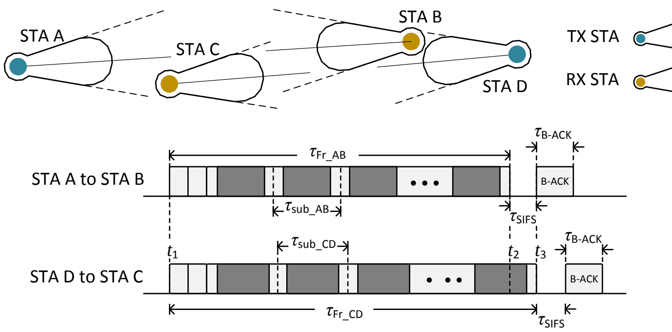

Fig. 4. A typical scenario of mainlobe-mainlobe interference and the enabled parallel transmissions.

between BIs so as to find the best rate in the long run. The detailed method of mapping the SIR and MCS are out of the scope of this study. We assume that after beamforming training and all necessary measurements, PCP/AP knows the appropriate MCS when parallel transmissions are carried out.

It is worth noting that if the interference takes place via MM connections, the SIR (cf. (7)) is normally too low for carrying out valid concurrent transmissions if the pathloss of the signal link and interference link are at the same level. To the best of our knowledge, no study explicitly allows STAs which are interfering each other with MM connections to transmit at the same time.

B. CTMAC principle

CTMAC enhances the IEEE 802.11ad by enabling the concurrent transmission in the main beam. Although CTMAC is targeted for the IEEE 802.11ad standard, its principle can be used for any wireless networks which have good directivity. It is well known that RTS-CTS-DATA-ACK four-way handshakes is not efficient in directional only networks because of the repetitively transmitted directional RTS and the prolonged carrier sensing time [10], [14]. Therefore, only the DATA-ACK two-way handshake is considered in this paper. A typical mainlobe-to-mainlobe (MM) interference topology is shown in the upper part of Figure 4, where two pairs of STAs are going to communicate. We first assume that STA A is scheduled to transmit to STA B with frame aggregation. As shown in the lower part of Figure 4, STA A starts transmitting to STA B at t_1, and stops transmitting at t_2. Afterwards STA B replies with a block ACK frame which contains the acknowledgements of all MPDUs in the received AMPDU. The block ACK starts being transmitted at t_3. The duration $\tau_{\text{Fr\_AB}}$ is the transmission duration of the AMPDU, and $\tau_{\text{B-ACK}}$ represents the transmission duration of the block ACK.

According to the interference topology, the AMPDU transmission from STA A and block ACK transmission from STA B generate different levels of interference to their neighboring node. STA A causes SM interference towards STA C and MM interference towards STA D. Because STA B is receiving, STA C may cause MM interference and STA D may cause SM interference towards STA B if they start transmitting. After transmitting AMPDU, STA B transmits a block ACK back to STA A. During the block ACK transmission, STA B causes MM interference towards STA C and causes SM interference towards STA D. If we follow the same principle that only allows parallel transmissions under the SS and SM interference scenarios, no transmission between STA C and STA D is able to be carried out. However, if the transmission between STA D and STA C are carried out following the lower part of Figure 4, parallel transmissions are feasible because no MM interference is generated between any two STAs. This way, the throughput is significantly increased.

C. Adaptive frame aggregation

Transmitting with the highest possible MCS can optimize the performance of the parallel transmitting STAs. However, STA pairs may transmit with different MCSs due to the different SIR values. Therefore, if two transmitting STAs transmit the same number of MPDU with different data rate, one STAs may stop first and wait for transmitting its block ACK frame. Obviously, it wastes spectrum resources. Hence, the most efficient strategy is that we select the number of MPDU so as to minimize the differences between the transmission time of both pairs. If the number of MPDU of one pair N_1 is given, then the number of MPDU of another pair N_2 can be calculated as,

$$N_2 = \underset{N_2}{\operatorname{argmin}} |\tau_{\text{Fr\_AB}} - \tau_{\text{Fr\_CD}}| \quad (8)$$

$$= \underset{N_2}{\operatorname{argmin}} |N_1 \tau_{\text{sub\_AB}} - N_2 \tau_{\text{sub\_CD}}| \quad (9)$$

$$= \underset{N_2}{\operatorname{argmin}} |N_1 \frac{L_{\text{MPDU}}}{R_1} - N_2 \frac{L_{\text{MPDU}}}{R_2}| \quad (10)$$

where $\tau_{\text{Fr\_AB}}$ and $\tau_{\text{Fr\_CD}}$ are the transmission time of a AMPDU sent by STA A and STA D, respectively. According to the SIR measurement results, the data rate of STA A and STA D are R_1 and R_2. The length of MPDU is L_{MPDU} bits.

IV. Simulation Results

In order to evaluate the performance of CTMAC, a number of simulations are carried out in a customized MATLAB simulator. The system configurations used in our simulations are selected according to the IEEE 802.11ad OFDM PHY specifications. In the simulations, we only consider LOS channels in a typical indoor environment with path loss exponent 2.25, which is set according to the channel model in [20] and the measurement results in [4]. The SNR and MCS mapping are set according to the results in [21] where the single input single output (SISO) packet error rate (PER) performance of all 802.11ad MCS versus the SNR for the LOS channels are given. In the following simulations, STAs are allowed to communicate with a certain MCS when the corresponding PER is lower than 1%. AMPDU scheme is applied in all simulations with N sub MPDUs. All simulations were repeated more than 10000 times to ensure the stability. In all simulations, we compare the CTMAC performance with

TABLE I
SIMULATION PARAMETERS

T_c SC chip time	0.57ns
T_{preamble}	$3328 \times T_c$
PLCP header	64bits
MAC header	288bits
AMPDU delimiter	32bits
Padding	16bits
MSDU length	7920Bytes
ACK payload	$8 \times N^*$Bytes
t_{SIFS}	$3\mu s$
t_{DIFS}	$13\mu s$
OFDM PHY data rate	MCS 15-24

* Number of MPDUs in AMPDU

and without adaptive frame aggregation algorithm and the original IEEE 802.11ad standard which allows no parallel transmissions. Several key parameters used in the simulations are listed in Table I.

Because the antenna directivity and the length of frame aggregation are the two key factors can impact CTMAC performance, we performed four simulations to investigate the relations between CTMAC and them. In all simulations, the goodput of two pairs of STAs which are in the mainlobes of each other as shown in Figure 4. We assume that STA A and STA D has infinite data to transmit to STA B and STA C, respectively. We randomly allocate two pairs of STAs in a line and ensure that all STAs are in the communication range of each other with the lowest MCS under the MM topology.

The directivity of the deployed antenna can significantly impact CTMAC performance. High gain in the mainlobe may enhance the SIR at the receiving STA and low gain in the sidelobe can reduce the interference level. In the first simulation, we evaluate the performance of CTMAC with different antenna radiation efficiencies which is defined in Section III. As shown in Figure 5(a), the goodput of CTMAC increases fast as the radiation efficiency increases and the enhancement is converging to 2-fold if the radiation efficiency is close to 1, i.e., nearly no transmission power is able to leak through the sidelobes. In this case, nearly no interference can be received through sidelobe so the two pairs are almost communicating independently. We also see that when the radiation efficiency is too small, e.g., less than 0.1, the performance of CTMAC is lower than the original IEEE 802.11ad MAC because the high interference level.

We also evaluate the performance of CTMAC with different beamwidth which is another important factor of antenna directivity. As shown in Figure 5(b), the goodput of the two pairs of STAs decreases rapidly as the beamwidth increases. It is owing to the fact that large beamwidth leads to small directional gain and high interference level through sidelobes. We also notice that the performance of CTMAC is worse than the original IEEE 802.11ad MAC when the beamwidth is greater than unit70° which is greater than most of the commercial-of-the-shelf (COTS) mm-Wave antennas.

The number of subframes in the frame aggregation scheme is another key configuration of CTMAC. We carried out a

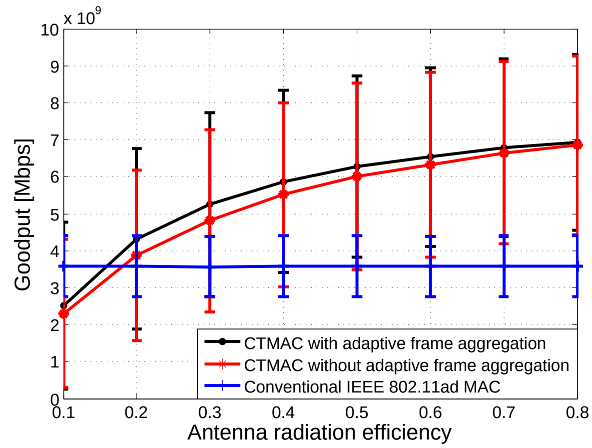

(a)

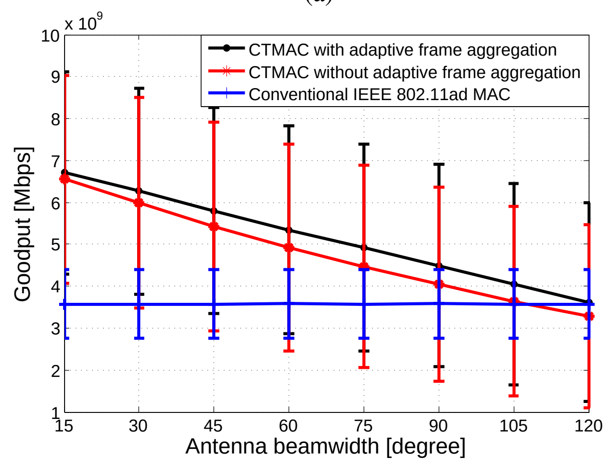

(b)

Fig. 5. (a) Achieved goodput with respect to the antenna radiation efficiency. The beamwidth of the antenna is 30°, the number of MPDUs in a AMPDU is 20. (b) Achieved goodput with respect to the antenna beamwidth. The beamwidth of the antenna is varying from 15° to 120°. The radiation efficiency is 0.5, and the number of MPDUs in a AMPDU is 20.

simulation to investigate the relations between the number of MPDUs in a AMPDU and the goodput of two STA pairs. As shown in Figure 6(a), the performances of the original IEEE 802.11ad MAC and CTMAC increase as the number of MPDUs increases. It's due to the fact that more MPDUs can lower down the overhead in both PHY layer and MAC layer. It is worth noting that in the realistic deployment, the length of frame aggregation scheme should be determined by jointly considering the channel conditions and packet error rate together.

In the last simulation, we evaluate the performance of CTMAC with the different MSDU length. As shown in Figure 6(b), the performance of all tested schemes increase when the MSDU length increases. The performance of CTMAC dominates the original IEEE 802.11ad MAC with all simulated MSDU length.

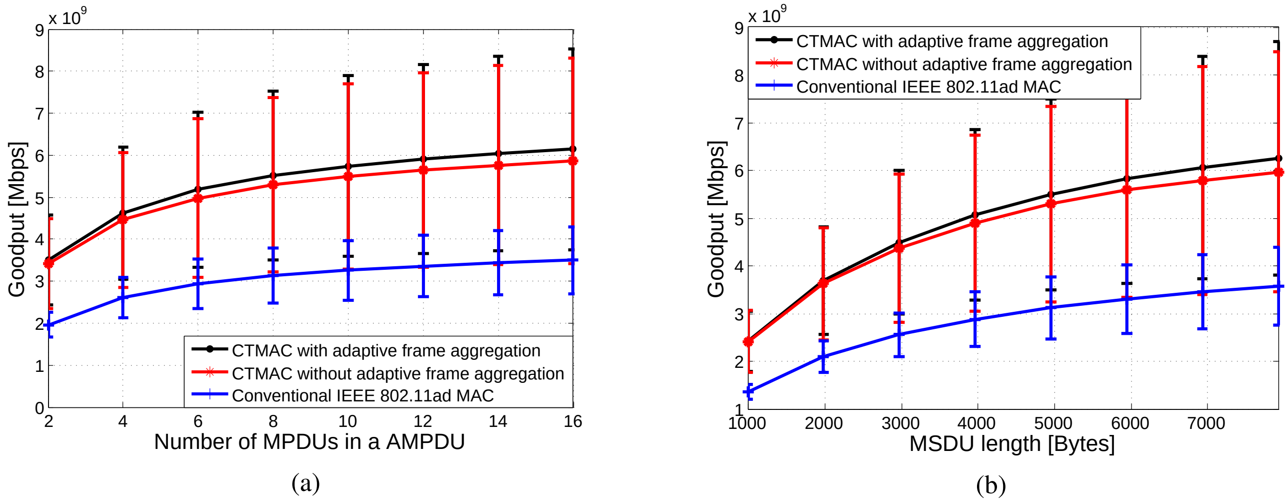

Fig. 6. (a) Achieved goodput with respect to the number of MPDUs in a AMPDU. The beamwidth of the antenna is 30°. The radiation efficiency is 0.5, and the number of MPDUs in a AMPDU is varying from 2 to 16. (b) Achieved goodput with respect to the length of MSDU. The beamwidth of the antenna is 30°. The radiation efficiency is 0.5, and the number of MPDUs in a AMPDU is 20. The length of the MSDU is varying from 990Bytes to 7920Bytes.

V. Conclusions

In this paper, we have presented the design and implementation of a novel directional MAC protocol, CTMAC, which enables STAs to carry out parallel transmissions even when their mainlobes are pointing to each other. By using a packet level scheduling algorithm with an adaptive frame aggregation scheme, CTMAC completely avoids the interference between mainlobes and optimizes the data transmission. This way, CTMAC achieves the parallel transmissions even under the strongest interfered topologies. It proves that directional transmission technologies have a great potential to enhance the spatial reuse of mm-Wave wireless networks. The numeric results show that CTMAC can significantly outperform the original IEEE 802.11ad MAC up to 2-fold.

References

[1] N. Guo, R.C Qiu, S.S Mo and K. Takahashi. 60-GHz Millimeter-Wave Radio: Principle, Technology, and New Results. *EURASIP Journal on Wireless Communications and Networking*, 2007(1):48–48, 2007.

[2] R.C. Daniels, J.N. Murdock, T.S. Rappaport and R.W. Heath. 60 GHz Wireless: Up Close and Personal. *IEEE Microwave Magazine*, 11(7):44–50, 2010.

[3] K. Haneda, J. Järveläinen, A. Karttunen, M. Kyrö and J. Putkonen. Indoor short-range radio propagation measurements at 60 and 70 GHz. In *European Conference on Antennas and Propagation*, pages 634–638, Hague, Netherlands, 2014.

[4] T.S. Rappaport, E. Ben-Dor, J.N. Murdock and Y-J. Qiao. 38 GHz and 60 GHz Angle-Dependent Propagation for Cellular & Peer-to-Peer Wireless Communications. In *IEEE International Conference on Communications*, pages 4568–4573, Ottawa, Canada, 2012.

[5] R.J. Weiler, M. Peter, W. Keusgen and M. Wisotzki. Measuring the Busy Urban 60 GHz Outdoor Access Radio Channel. In *IEEE International Conference on Ultra-Wideband*, pages 166–170, Paris, France, 2014.

[6] J. Lu, D. Steinbach, P. Cabrol, P. Pietraski and R.V. Pragada. Propagation Characterization of an Office Building in the 60 GHz Band. In *European Conference on Antennas and Propagation*, pages 809–813, Hague, Netherlands, 2014.

[7] J. Ansari, N. Perpinias, A. Nahring, P. Mähönen and M. Petrova. Empirical Characterization of mm-wave Communication Links in Realistic Indoor Scenarios. In *IEEE Wireless Communications and Networking Conference*, pages 1799–1804, New Orleans, LA, USA, 2015.

[8] Q. Chen, J.Q. Tang, D.T.C. Wong, X.M. Peng and Y.G. Zhang. Directional Cooperative MAC Protocol Design and Performance Analysis for IEEE 802.11 ad WLANs. *IEEE Transactions on Vehicular Technology*, 62(6):2667–2677, 2013.

[9] P-.P. Xu and H-.Y. Chu. A novel link scheduling strategy for concurrent transmission in mmWave WPANs based on beamforming information. In *IEEE Wireless Communications and Networking Conference*, pages 1709–1714, 2014.

[10] P. Wang, M. Petrova, and P. Mähönen. Coop-DMAC: A Cooperative Directional MAC Protocol for Wireless Networks. In *IEEE International Symposium on a World of Wireless Mobile and Multimedia Networks*, pages 1–9, 2015.

[11] Y-.X. Lin and V.WS. Wong. Frame Aggregation and Optimal Frame Size Adaptation for IEEE 802.11 n WLANs. In *IEEE Global Telecommunications Conference*, pages 1–6. IEEE, 2006.

[12] B. Ginzburg and A. Kesselman. Performance Analysis of A-MPDU and A-MSDU Aggregation in IEEE 802.11n. In *IEEE Sarnoff symposium*, pages 1–5. IEEE, 2007.

[13] C. Shin, H. Park and H.M. Kwon. PHY-Supported Frame Aggregation for Wireless Local Area Networks. *IEEE Transactions on Mobile Computing*, 13(10):2369–2381, 2014.

[14] O. Bazan, and M. Jaseemuddin. A survey on MAC protocols for wireless adhoc networks with beamforming antennas. *IEEE Communications Surveys & Tutorials*, 14(2):216–239, 2012.

[15] L.X. Cai, L. Cai, X-.M. Shen and J.W. Mark. REX: A randomized EXclusive region based scheduling scheme for mmWave WPANs with directional antenna. *IEEE Transactions on Wireless Communications*, 9(1):113–121, 2010.

[16] R. Ramanathan. On the Performance of Ad Hoc Networks with Beamforming Antennas. In *ACM international symposium on Mobile ad hoc networking & computing*, pages 95–105. ACM, 2001.

[17] IEEE Standard for Definitions of Terms for Antennas. *IEEE Std 145-2013 (Revision of IEEE Std 145-1993)*, pages 1–50, March 2014.

[18] Flann Microwave. Antennas: Standard Gain Horn, http://www.flann.com, Last Visited: 02.09.2015.

[19] D. Halperin, W-.j. Hu, A. Sheth and D. Wetherall. Predictable 802.11 packet delivery from wireless channel measurements. *ACM SIGCOMM Computer Communication Review*, 41(4):159–170, 2011.

[20] A. Maltsev. Path Loss Model Development for TGad Channel Models, https://mentor.ieee.org/802.11/dcn/09/11-09-0553-01-00ad-path-loss-model-development-for-tgad-channel-models.ppt, Last Visited: 02.09.2015.

[21] X-.Y. Zhu, A. Doufexi and T. Kocak. A performance evaluation of 60 GHz MIMO systems for IEEE 802.11 ad WPANs. In *IEEE 22nd International Symposium on Personal Indoor and Mobile Radio Communications*, pages 950–954. IEEE, 2011.